PI3Kγ activates MLCK210 to promote integrin activation, leading to tumor inflammation and progression

Michael C. Schmid[1], Sang Won Kang[2], Megan J. Kaneda[1], D. Martin Watterson[3] and Judith A. Varner[1,4]

[1]Moores Cancer Center, University of California, San Diego, La Jolla, CA

[2]Division of Life and Pharmaceutical Science, Ewha Woman's University, Seoul Korea

[3]Department of Pharmacology, Northwestern University, Chicago, IL

[4]Department of Pathology and Medicine, University of California, San Diego, La Jolla, CA; to whom correspondence should be addressed: jvarner@ucsd.edu

Abstract

Myeloid cells play key roles in cancer immune suppression and progression. In response to tumor derived factors, myeloid cell integrins undergo conformational changes, or activation, which promotes cell extravasation and tumor inflammation. Chemokines, cytokines and interleukins stimulate PI3Kγ-mediated Rap1 activation, leading to conformational changes in integrins that promote extravasation and tumor inflammation. Here we show that PI3Kγ activates a high molecular weight form of myosin light chain kinase, MLCK210, that promotes myosin-dependent Rap1 GTP loading and subsequent integrin activation. Genetic or pharmacological inhibition of MLCK210 suppressed integrin activation, myeloid cell adhesion and migration, tumor inflammation and tumor progression. These results demonstrate a critical role for MLCK210 in tumor inflammation and serve as basis for the development of new approaches to develop immune oncology therapeutics.

Introduction

Inflammation contributes to infectious, cardiovascular, autoimmune, and neurodegenerative diseases and cancer[1]. Vascular endothelial cells and myeloid cells (monocytes, macrophages and neutrophils) play critical roles in inflammatory responses. Myeloid cells invade inflamed tissues, where they can contribute to pathology by expressing inflammatory mediators, reactive oxygen species, angiogenic factors and immunosuppressive factors[2]. Endothelial cells respond to inflammatory stimuli by promoting myeloid cell adhesion and extravasation, by becoming more permeable and by undergoing angiogenesis[3]. Sustained recruitment of inflammatory cells to tissues can lead to progressive damage induced by release of oxygen radicals, which can lead to the development of cancer[4]. Targeting the mechanisms controlling myeloid cell responses to inflammatory stimuli could lead to new approaches to suppress chronic inflammation and cancer.

A variety of inflammatory factors released by damaged tissues activate G protein coupled receptors (GPCRs), receptor tyrosine kinases (RTKs) or Toll-like receptor/interleukin1 receptor family members (TLR/IL1Rs) to initiate myeloid cell recruitment during inflammation.[5] Integrin activation depends on Rap1 (Ras-proximate-1), a Ras-like small GTP-binding protein and its effector protein RIAM, which localizes talin to the membrane.[6-7] Talin binds integrin β chain cytoplasmic tails, inducing a shift in the conformation of the extracellular domain of the integrin and resulting in an allosteric increase in ligand-binding affinity.[8] Paxillin binding to the integrin α4 cytoplasmic tail promotes $\alpha 4$ integrin activation, adhesion and trafficking of lymphocytes and myeloid cells[9-10]. We previously found that inflammatory stimuli promote integrin α4β1 activation, cell adhesion and myeloid cell trafficking[11] by activating a single PI3K isoform, PI3Kγ[12]. PI3Kγ mediated integrin activation requires PLCγ, which cleaves phospholipids to produce Ca2+ and diacylglycerol (DAG), the DAG-activated RapGEFs, CalDAG-GEFI and II, Rap1a and RIAM,

thereby activating integrin $\alpha 4\beta 1$ in a RIAM-dependent manner[11-12]. Pharmacological or genetic blockade of PI3Kγ or integrin α4β1 suppressed adhesion and recruitment of both monocytes and granulocytes into tumors and inhibited disease progression.[11-12] These findings indicate that targeting inflammation might provide significant benefit in the treatment of a wide variety of diseases.

Deciphering the molecular mechanisms by which myeloid cell integrins are activated could lead to the development of new approaches to treat acute and chronic inflammatory and vascular diseases. Here we show that PI3Kγ activates a high molecular weight form of myosin light chain kinase, MLCK210, and myosin to promote Rap1 GTP loading and integrin conformational changes that promote tumor inflammation progression. These studies also identify MLCK210 inhibitors as potential immune oncology therapeutics.

Results

MLCK210 colocalizes with integrin α4β1

We previously determined that tumor derived growth factors and chemokines promote PI3Kγ mediated integrin α4β1 conformational changes during tumor inflammation[11]. To identify proteins that closely associate with myeloid cell integrin α4β1 during its activation, we stimulated primary myeloid cells with Lewis Lung carcinoma tumor cell condition medium (TCM) or basal media, solubilized cells and immunoprecipitated integrin α4β1. We then performed silver-staining and immunoblotting to detect integrin α4β1 interacting proteins (Figure 1A). Immunoblotting revealed that paxillin and talin co-immunoprecipitated with integrin α4β1 upon stimulation with TCM (Figure 1A). Silver staining identified co-precipitating proteins with molecular weights of 80 kDa and 210 kDa upon stimulation with TCM but not under basal conditions (Figure 1A; Supplementary Figure 1A). Proteomic analysis identified the 80kDa protein as Gelsolin and the 210 kDa protein as a high molecular weight form of myosin light chain kinase (MLCK210), a key regulator of vascular permeability[13-18] (Supplementary Figure 1A). Gelsolin is an actin-filament severing and capping protein in podosomes that is inhibited by PIP3, the product of PI3Kinases[19]. MLCK210 is an alternatively spliced MLCK isoform that contains the entire 108 kDa non-muscle MLCK protein as well as six N-terminal IgG-C2-like domains and two tandem DXR actin-binding domains (Figure 1C)[13-18]. MLCKs contain a core catalytic domain and a calmodulin-sensitive auto-inhibitory domain that folds back on the catalytic domain to inhibit kinase activity. Upon activation by calmodulin, MLCK phosphorylates Myosin Light Chain (MLC), thereby stimulating myosin ATPase[20]. As activated myosin undergoes a conformational change that allows it to cyclically bind and release actin filaments, it promotes contractility that leads to cell shape change and migration[21].

To confirm whether MLCK210 and integrin α4β1 colocalize in myeloid cells, integrin α4 was immunoprecipitated from unstimulated and SDF-1α stimulated myeloid cells isolated from WT or

Figure 1

a

IP: Integrin α4β1

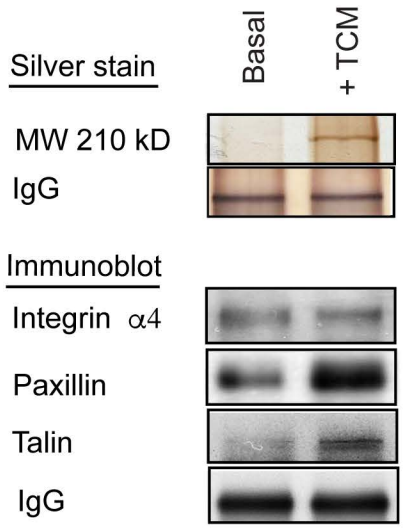

b

Tandem Mass Spectrometry

Protein name (swiss prot no. or TrEMBL no)	Residue number	Peptide sequence
Myosin, light polypeptide kinase (B1B1A8)	33-49 1239-1554	VSSMPLTEAPAFILPPR SSLPPVLGTESDATVK
Gelsolin (P13020)	583-595 712-726	SGALNSNDAFVLK DSQEEEKTEALTSAK

c

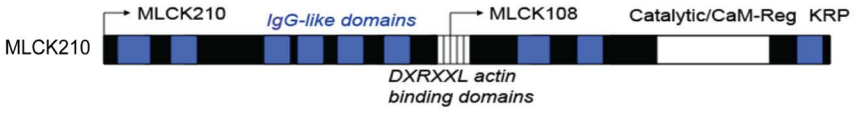

d

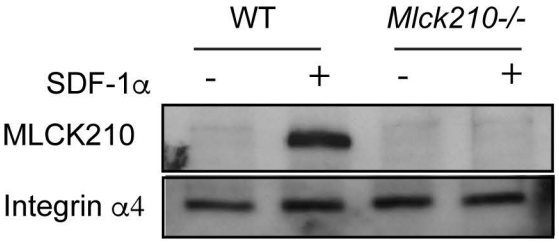

e

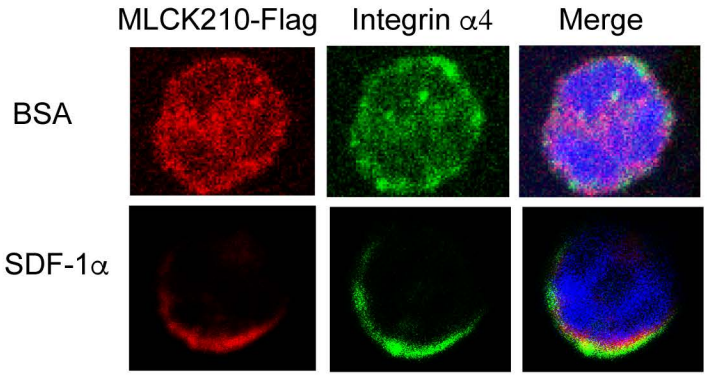

f

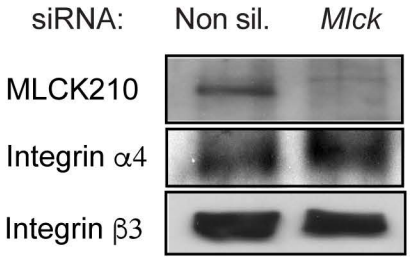

g

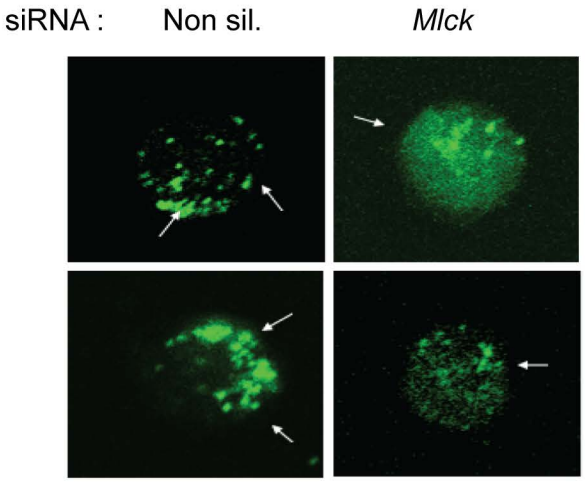

Integrin α4

Figure 1: MLCK210 is an integrin α4β1 associated protein. (A) Integrin α4β1 immunoprecipitates from TCN stimulated or unstimulated CD11b+ myeloid cells were silver stained or immunoblotted. Upper: A co-immunoprecipitated 210 kDa protein as well as IgG were detected by silver staining. Integrin α4, paxillin, talin and IgG were detected by immunoblotting. (B) Peptide sequences of the 80 kDa and 210kDa proteins co-immunoprecipitated with integrin α4β1 were identified gelsolin and as a high molecular weight isoform of myosin light chain kinase, MLCK210, respectively. (C) Schematic depicting the structure of MLCK210. (D) Immunoprecipitates of integrin α4 from unstimulated and SDF-1α stimulated WT and *Mlck210-/-* myeloid cells were immunoblotting to detect MLCK210 and the integrin α4 subunit. (E) Immunofluorescence detection of integrin α4 (green) and Flag-tagged MLCK210 (red) in Flag-MLCK210 transfected myeloid cells that were incubated with SDF-1α and BSA coated beads. Nuclei were detected with Dapi (blue). (F) Detection of MLCK210 in immunoblots from lysates of *Mlck* and non-silencing siRNA transfected myeloid cells. (G) Integrin α4 clustering (green, arrows) by SDF1α coated beads in *Mlck* and non-silencing siRNA transfected myeloid cells.

Mylk210-/- mice, in which the alternatively transcribed MLCK210 isoform of MLCK was selectively deleted[16]. SDF1a was used as to stimulate integrin activation as we had previously found it is abundantly expressed by LLC cells and that it promotes integrin mediate adhesion in vitro[11]. Integrin α4 immunoprecipitates were immunoblotted to detect MLCK and integrin α4. We found that, MLCK210 co-precipitated with integrin α4 in SDF-1 stimulated wildtype (WT) but not *Mlck210-/-* cells and not in unstimulated cells (Figure 1D). To determine whether MLCK210 and integrin α4β1 colocalize in intact myeloid cells, myeloid cells were transfected with Flag-tagged MLCK210, incubated with SDF-1α or BSA coated beads, fixed, permeabilized and analyzed for colocalization of Flag-tagged MLCK210 (red) and integrin α4 (green) by immunofluorescence microscopy. SDF-1α but not BSA coated beads induced co-clustering of MLCK210 (red) and integrin α4 (green) at the plasma membrane (Figure 1E). To test the dependence of integrin α4 clustering (green, arrows) on MLCK210, myeloid cells were transfected with non-silencing or *Mlck* siRNA (Figure 1F), then incubated with SDF-1α coated beads. SDF- 1α beads induced integrin clustering in control but not *Mlck* knockdown cells (Figure 1G). Together, these results demonstrate that MLCK210 co-localizes with integrin α4 and is required for integrin clustering in response to chemokine stimulation.

MLCK210 is required for integrin α4β1-mediated cell adhesion

We previously demonstrated that integrin α4β1 mediates cytokine and chemokine stimulated myeloid cell adhesion to vascular cell adhesion molecule 1 (VCAM-1) on endothelium[11]. To determine whether MLCK210 is required for integrin α4-mediated adhesion, *Mlck210*-/- and WT myeloid cells were incubated with basal medium or medium containing IL-1β, IL-6, SDF-1, TNFα, VEGF-A or Lewis lung carcinoma cell conditioned medium (TCM). Cells were then allowed to adhere to endothelial cell monolayers (HUVEC) or to recombinant soluble VCAM-1 coated on plastic plates (Figure 2a). While cytokine stimulated WT myeloid cells adhered to HUVEC and

Figure 2

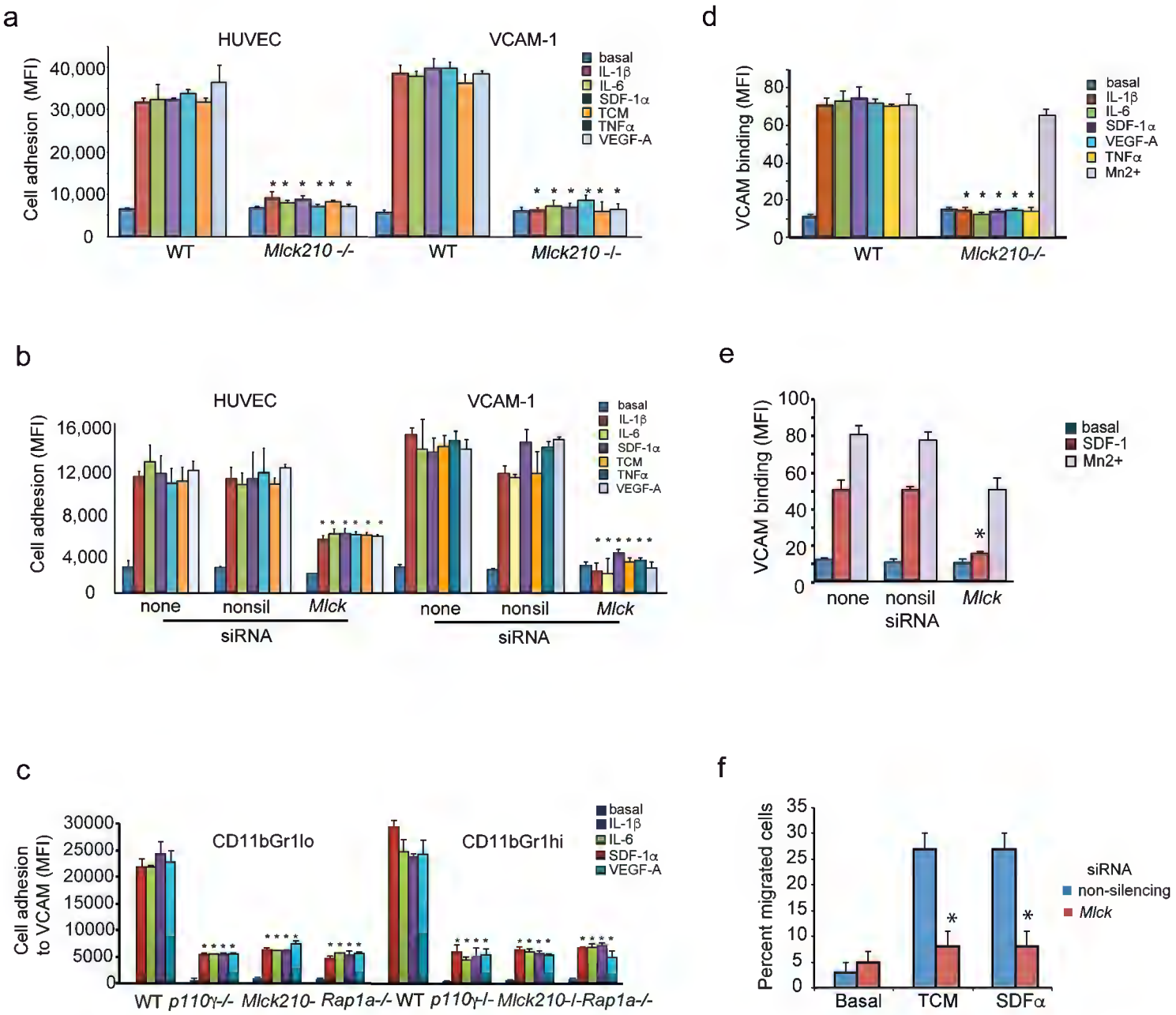
a
HUVEC
VCAM-1
Cell adhesion (MFI)
40,000
30,000
20,000
10,000
0
basal
IL-1β
IL-6
SDF-1α
TCM
TNFα
VEGF-A
WT
Mlck210 -/-
WT
Mlck210 -/-
d
VCAM binding (MFI)
80
60
40
20
0
basal
IL-1β
IL-6
SDF-1α
VEGF-A
TNFα
Mn2+
WT
Mlck210-/-
b
HUVEC
VCAM-1
Cell adhesion (MFI)
16,000
12,000
8,000
4,000
0
basal
IL-1β
IL-6
SDF-1α
TCM
TNFα
VEGF-A
none
nonsil
Mlck
none
nonsil
Mlck
siRNA
siRNA
e
VCAM binding (MFI)
100
80
60
40
20
0
basal
SDF-1
Mn2+
none
nonsil
Mlck
siRNA
c
Cell adhesion to VCAM (MFI)
30000
25000
20000
15000
10000
5000
0
CD11bGr1lo
CD11bGr1hi
basal
IL-1β
IL-6
SDF-1α
VEGF-A
WT
p110γ-/-
Mlck210-
Rap1a-/-
WT
p110γ-/-
Mlck210-/-
Rap1a-/-
f
Percent migrated cells
35
30
25
20
15
10
5
0
siRNA
non-silencing
Mlck
Basal
TCM
SDFα

Figure 2: MLCK210 promotes integrin α4 mediated myeloid cell adhesion. (A) Adhesion expressed as mean fluorescence intensity (MFI) of cytokine- and tumor conditioned medium (TCM)-stimulated WT or *Mlck210*-/- myeloid cells to HUVEC or VCAM. (B) Adhesion of cytokine-stimulated control, control-transfected (Nonsil), or *Mlck* siRNA-transfected myeloid cells to HUVEC or VCAM. (C) Adhesion of CD11bGr1^{lo} monocytes and CD11bGr1^{hi} granulocytes from WT, *p110γ-/-, Mlck210-/-* or *Rap1a-/-* mice to purified VCAM-1 coated plates. (D-E) VCAM-Fc binding (MFI) to basal medium, SDF-1α and Mn^{2+} stimulated myeloid cells from (D) *Mlck210-/-* mice or (E) *Mlck210* siRNA transfected cells. (F) Migration of *Mlck210* or control siRNA transfected myeloid cells toward basal medium, SDF-1α or tumor cell conditioned medium (TCM). Data are represented as mean +/- SEM; n=4 for all conditions, $p<0.05$ unless otherwise defined.

VCAM-1, *Mlck210*-/- myeloid cells did not (Figure 2A). Deletion of *Mlck210* did not affect adhesion of myeloid cells to any other substrate (Supplementary Figure 1B). In support of these findings, MLCK siRNA-treated myeloid cells exhibited poor adhesion to HUVEC and VCAM, in contrast to control siRNA transfected cells (Figure 2B). Previously, we showed that integrin $\alpha 4$-mediated adhesion of $Gr1^{lo}$ monocytes and $Gr1^{hi}$ granulocytes to endothelium required the activity of both PI3Kγ and $Rap1^{ref}$. As both CD11b+$Gr1^{lo}$ monocytes and CD11b+$Gr1^{hi}$ granulocytes extravasate into tumors from peripheral blood, we asked whether the adhesion of each of these two cells types was similarly regulated by PI3Kγ, Rap1, and MLCK210. We found that the adhesion (MFI) of both CD11b$Gr1^{lo}$ monocytes and CD11b$Gr1^{hi}$ granulocytes from *p110γ-/-, Mlck210-/-* or *Rap1a-/-* mice to VCAM-1 coated plates was strongly inhibited compared to the adhesion of cytokine stimulated WT cells (Figure 2C). These results indicate that MLCK210 could play a key role in the PI3Kγ-Rap1 pathway that promotes integrin $\alpha 4$ mediated adhesion.

To determine if MLCK210 controls integrin activation, unstimulated and cytokine-stimulated WT and *Mlck210*-/- myeloid cells were incubated with recombinant VCAM-1 conjugated to the Fc portion of the immunoglobulin heavy chain and then with anti-Fc fluorochrome-conjugated antibody. VCAM-Fc bound to cytokine-stimulated WT but not *Mlck210-/-* cells (Figure 2D), while Mn2+, which independently activates integrins by establishing a salt bridge with ligands[22], stimulated VCAM Fc binding independently of cytokine stimulation (Figure 2D). VCAM-Fc binding to SDF-1α stimulated myeloid cells was also suppressed in *Mlck210* but not control siRNA transfected cells (Figure 2E). Additionally, migration of myeloid cells toward SDF-1α or tumor cell conditioned medium (TCM) was impaired in *Mlck210* but not control siRNA transfected cells (Figure 2F).

Figure 3

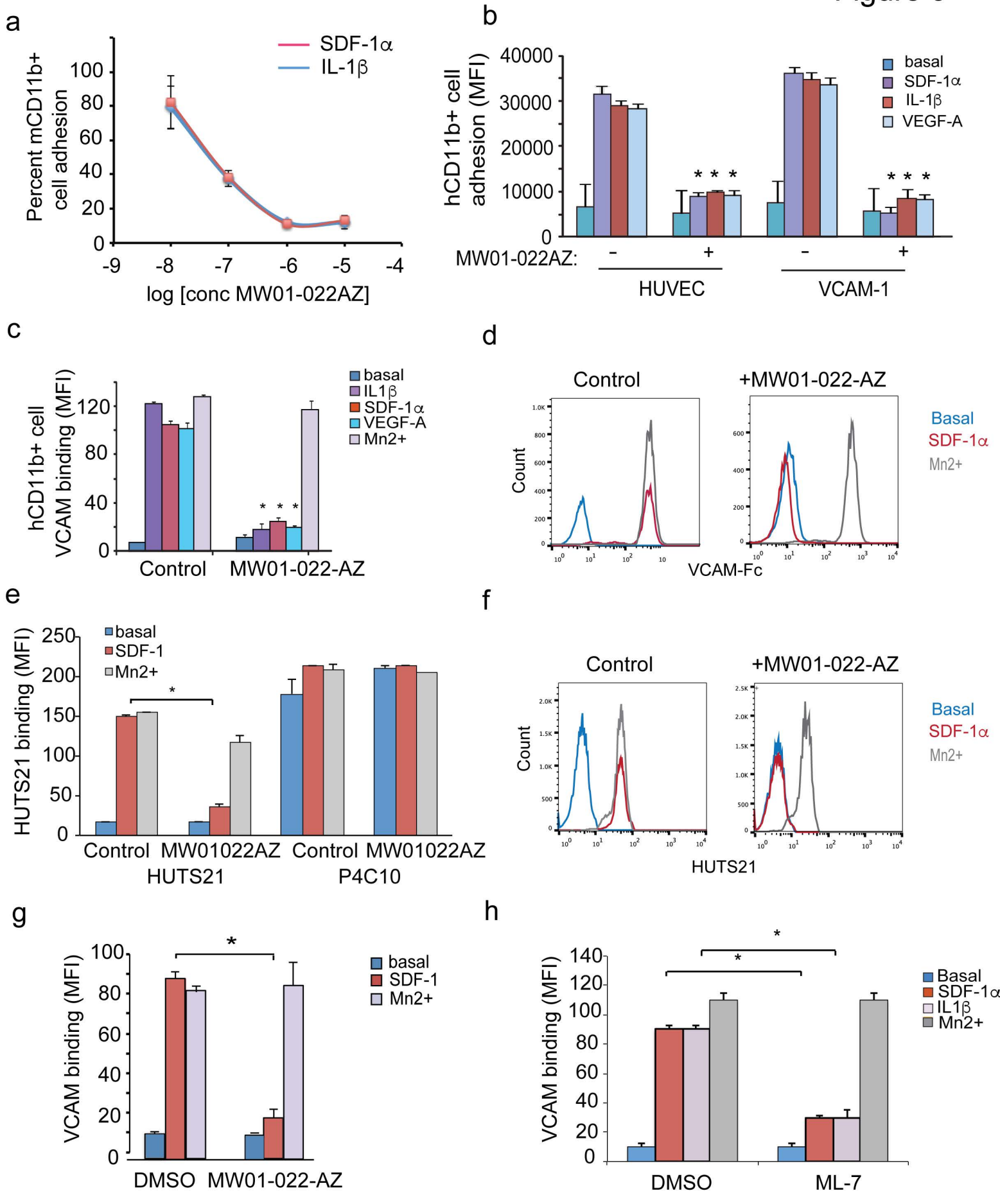
a
SDF-1α
IL-1β
Percent mCD11b+ cell adhesion
log [conc MW01-022AZ]
b
hCD11b+ cell adhesion (MFI)
basal
SDF-1α
IL-1β
VEGF-A
MW01-022AZ:
HUVEC
VCAM-1
c
hCD11b+ cell VCAM binding (MFI)
basal
IL1β
SDF-1α
VEGF-A
Mn2+
Control
MW01-022-AZ
d
Control
+MW01-022-AZ
Count
VCAM-Fc
Basal
SDF-1α
Mn2+
e
HUTS21 binding (MFI)
basal
SDF-1
Mn2+
Control
MW01022AZ
HUTS21
P4C10
f
Control
+MW01-022-AZ
Count
HUTS21
Basal
SDF-1α
Mn2+
g
VCAM binding (MFI)
basal
SDF-1
Mn2+
DMSO
MW01-022-AZ
h
VCAM binding (MFI)
Basal
SDF-1α
IL1β
Mn2+
DMSO
ML-7

Figure 3. MLCK210 inhibitor prevents integrin α4 activation. (A) Effect of MW01-022AZ on murine myeloid cell adhesion to VCAM-1 stimulated by SDF-1α or IL1β. (B) Effect of MW01-022AZ on cytokine-stimulated human myeloid cell adhesion to HUVEC or VCAM. (C) Quantification of VCAM-Fc binding to cytokine or Mn2+ stimulated human CD11b+ myeloid cells in the presence or absence of MW01-022AZ. (D) FAC profiles of VCAM-Fc binding to basal medium, SDF-1α and Mn2+ stimulated human myeloid cells. (E) Quantification of HUTS21 (activation epitope) or P4C10 (total β1) antibody binding to basal medium, SDF-1 or Mn2+ stimulated human CD11b+ cells in the presence or absence of MW01-022AZ. (F) FACs profiles of HUTS antibody binding to human myeloid cells stimulated with basal medium, SDF-1α and Mn2+ stimulated human myeloid cells in the presence or absence of MW01-022AZ. (G-H) VCAM binding to (G) MW-022AZ-treated or (H) ML-7-treated human myeloid cells stimulated with basal medium, SDF-1α and Mn2+. Data are represented as mean +/- SEM; n=4 for all conditions, $p<0.05$ unless otherwise defined.

To determine whether MLCK inhibitors could similarly suppress cytokine-mediated integrin activation and adhesion, WT myeloid cells were incubated with medium, SDF-1β, or IL-1β in the presence and absence of either ML-7 or MW01-022-AZ, two MLCK inhibitors (Figure 3A, Supplementary Figure 1C). We found that MLCK inhibitors suppressed SDF-1 and IL-1β induced adhesion of murine myeloid cells to VCAM-1 in a dose-dependent manner (Figure 3A; Supplementary Figure 1C). MW01-022-AZ also inhibited cytokine-stimulated human myeloid cell adhesion to HUVEC or VCAM (Figure 3A-B; Supplementary Figure 1C). MW01-022-AZ suppressed integrin activation, as it prevented VCAM-Fc binding to cytokine but not Mn2+ stimulated human CD11b+ myeloid cells (Figure 3C-D). MW01-022-AZ also inhibited binding of HUTS21, an antibody that selectively binds to activated but not inactive β1 integrins, but had no effect on binding of P4C10, an anti-β1 integrin antibody, to SDF-1 stimulated human myeloid cells (Figure 3E-F). MLCK inhibitors similarly suppressed integrin activation in murine myeloid cells, as MW01-022-AZ and ML-7 each prevented VCAM-Fc binding to cytokine stimulated murine myeloid cells (Figure 3G-H). Taken together, these results show that MLCK210 promotes integrin α4β1 activation in murine and human myeloid cells.

MLCK210 is required for Rap1 activation

Our previous studies showed that PI3Kγ promotes integrin activation and adhesion by promoting Rap1 activation. To determine if MLCK210 plays a role in integrin activation and adhesion upstream of PI3Kγ, we analyzed Akt phosphorylation in response to cytokine stimulation in WT and *Mlck210-/-* myeloid cells. Deletion of MLCK210 had no effect on Akt phosphorylation (Figure 4A). These results suggest that MLCK210 acts downstream of PI3Kγ. We next asked whether MLCK210 could play a role in Rap1 activation, as Rap1 activation is a late step in the signaling cascade leading to integrin activation[23]. Indeed, we found that Rap1 activation, as measured by GTP-loading, was impaired in SDF-1α stimulated *Mlck210-/-* but not WT myeloid cells (Figure

Figure 4

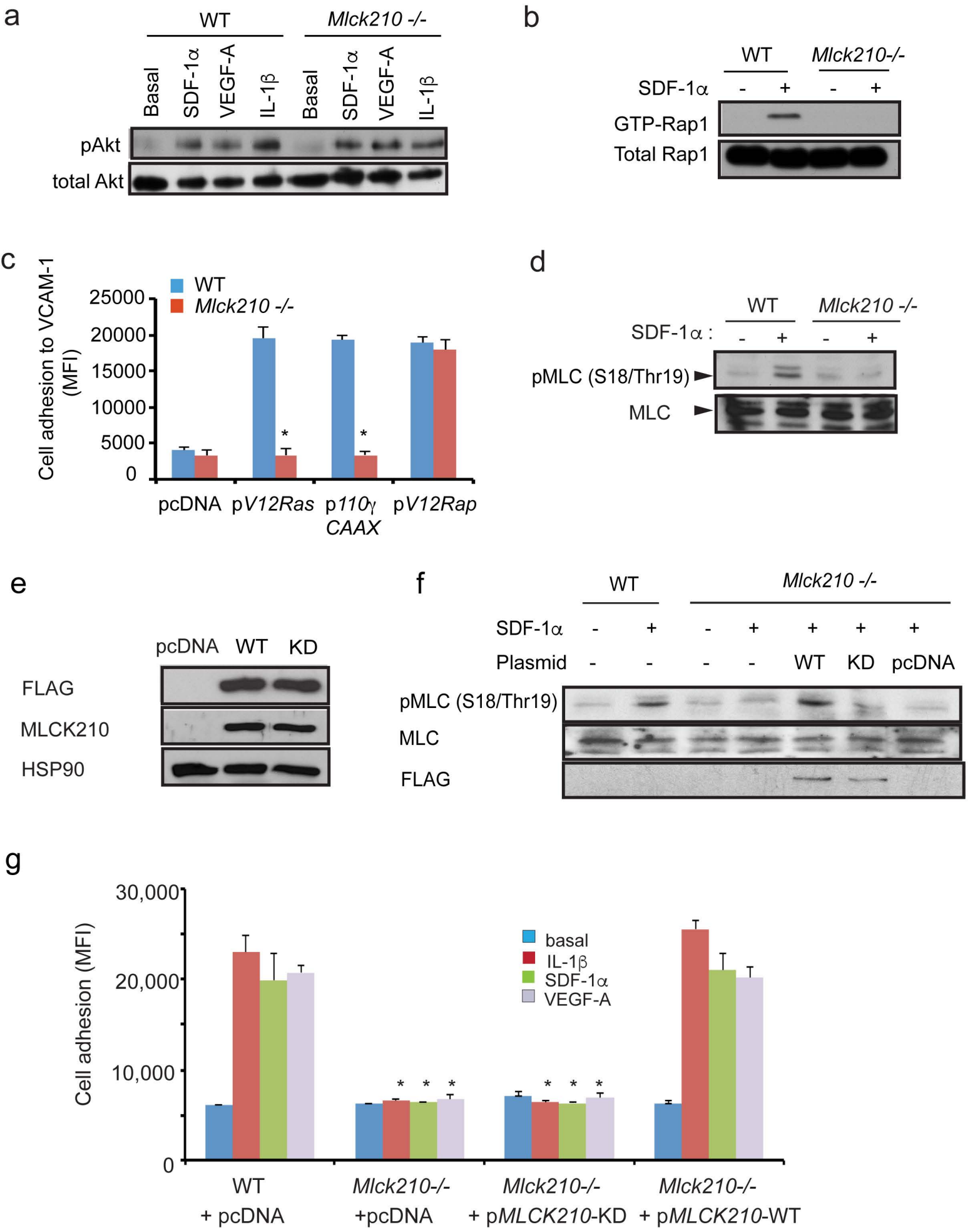
a
WT
Mlck210 -/-
Basal
SDF-1α
VEGF-A
IL-1β
Basal
SDF-1α
VEGF-A
IL-1β
pAkt
total Akt
b
WT
Mlck210-/-
SDF-1α
- + - +
GTP-Rap1
Total Rap1
c
WT
Mlck210 -/-
Cell adhesion to VCAM-1 (MFI)
25000
20000
15000
10000
5000
0
pcDNA
pV12Ras
p110γ CAAX
pV12Rap
d
WT
Mlck210 -/-
SDF-1α :
- + - +
pMLC (S18/Thr19)
MLC
e
pcDNA
WT
KD
FLAG
MLCK210
HSP90
f
WT
Mlck210 -/-
SDF-1α
- + - + + + +
Plasmid
- - - - WT KD pcDNA
pMLC (S18/Thr19)
MLC
FLAG
g
Cell adhesion (MFI)
30,000
20,000
10,000
0
basal
IL-1β
SDF-1α
VEGF-A
WT + pcDNA
Mlck210-/- +pcDNA
Mlck210-/- + pMLCK210-KD
Mlck210-/- + pMLCK210-WT

Figure 4: PI3Kgamma activates MLCK210 and Rap-mediated adhesion. (A) Akt phosphorylation in WT and *Mlck210*-/- cytokine stimulated myeloid cells. (B) Rap1 GTP loading in cytokine stimulated WT and *Mlck210-/-* myeloid cells. (C) Adhesion to VCAM of WT and *Mlck210-/-* myeloid cells after transfection with active Ras (G12VRas), active PI3Kγ (p110γCAAX) or active Rap (RapG12V). (D) Myosin Light Chain (MLC) S18/Thr19 phosphorylation in cytokine-stimulated WT and *Mlck210-/-* myeloid cells. (E) Immunoblotting to detect Flag-tagged MLCK210, total MLCK210 and HSP90 in WT myeloid cells and *Mlck210-/-* myeloid cells transfected with control (pcDNA) and MLCK210 expression plasmids. (F) Immunoblotting to detect phosphorylated MLC and total MLC in SDF1a stimulated or unstimulated WT or *Mlck210-/-* myeloid cells that had been transfected with control (pcDNA) or flag-tagged WT and Kinase dead (KD) MLCK210 expression plasmids. (G) Cytokine stimulated VCAM-1 adhesion of WT and *Mlck210*-/- myeloid cells that had been transfected with control (pcDNA), WT or Kinase Dead MLCK210 expression constructs. Data are represented as mean +/- SEM; n=4 for all conditions, $p<0.05$ unless otherwise defined.

4B). In previous studies, we observed that expression of activated Ras, PI3Kγ and Rap1 promoted integrin activation and adhesion in the absence of cytokine stimulation[7]. Importantly, we found that expression of activated Ras (RasG12V) or PI3Kγ (p110γCAAX) constitutively activated adhesion of WT but not *Mlck210-/-* myeloid cells, suggesting that MLCK210 is required for myeloid cell adhesion downstream of Ras and PI3Kγ (Figure 4C; Supplementary Figure 2). In contrast, expression of activated RapG12V stimulated α4β1-mediated adhesion in WT and in MLCK210 null myeloid cells (Figure 4C; Supplementary Figure 2), indicating that MLCK210 promotes integrin activation downstream of PI3Kγ and upstream of Rap.

Myosin promotes integrin activation

Since the major known substrate for all MLCK isoforms is myosin light chain (MLC), we investigated a role for myosin in integrin activation. MLC was phosphorylated in WT cells but not in *Mlck210-/-* cells (Figure 4D). MLCK210 catalytic activity is required for cytokine induced MLC phosphorylation in myeloid cells, as expression of Flag-tagged WT MLCK210 (WT), but not Flag-tagged kinase-dead MLCK210 (KD) or control DNA (pcDNA), could restore MLC phosphorylation to *Mlck210-/-* cells (Figure 4E-F). MLCK210 catalytic activity is also required for integrin mediated adhesion, since expression of catalytically active MLCK210 (WT), but not kinase-dead MLCK210 (KD), restored cytokine stimulated adhesion to VCAM in *Mlck210-/-* cells (Figure 4G). We found that catalytically active MLCK210 was required to promote cytokine induced co-localization and clustering of α4β1 and MLCK210, Rap1, and Paxillin (Supplementary Figure 3A). Taken together, these results indicate that MLCK210 acts downstream of PI3Kγ but upstream of Rap1 and plays a key role in promoting integrin α4 activation and clustering. MLCK can be activated by the influx of calcium ions, resulting in calmodulin-dependent MLCK activation[20]. To explore how MLCK210 becomes activated by PI3Kγ signaling, we evaluated the effects of the PKC inhibitor R0-32-0432 and the calcium/calmodulin inhibitor W7 on cytokine-mediated adhesion to VCAM. We found that

Figure 5

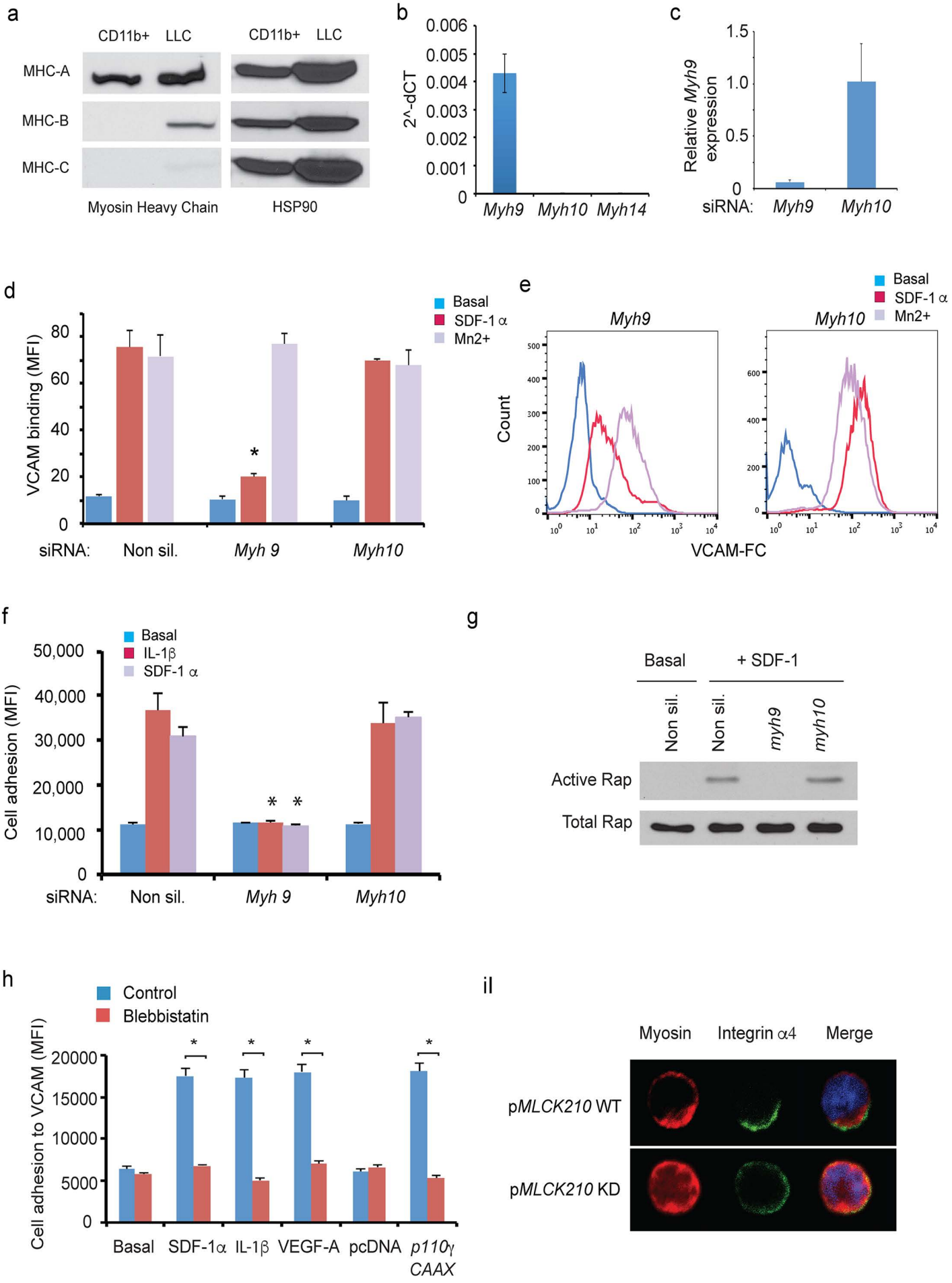
a
CD11b+
LLC
CD11b+
LLC
MHC-A
MHC-B
MHC-C
Myosin Heavy Chain
HSP90
b
2^-dCT
0.006
0.005
0.004
0.003
0.002
0.001
0
Myh9
Myh10
Myh14
c
Relative Myh9 expression
1.5
1.0
0.5
0
siRNA:
Myh9
Myh10
d
VCAM binding (MFI)
80
60
40
20
0
Basal
SDF-1 α
Mn2+
*
siRNA:
Non sil.
Myh 9
Myh10
e
Basal
SDF-1 α
Mn2+
Myh9
Myh10
Count
VCAM-FC
f
Basal
IL-1β
SDF-1 α
Cell adhesion (MFI)
50,000
40,000
30,000
20,000
10,000
0
* *
siRNA:
Non sil.
Myh 9
Myh10
g
Basal
+ SDF-1
Non sil.
Non sil.
myh9
myh10
Active Rap
Total Rap
h
Control
Blebbistatin
Cell adhesion to VCAM (MFI)
20000
15000
10000
5000
0
*
*
*
*
Basal
SDF-1α
IL-1β
VEGF-A
pcDNA
p110γ CAAX
il
Myosin
Integrin α4
Merge
pMLCK210 WT
pMLCK210 KD

Figure 5: MLCK and myosin in myeloid cells. (A) Immunoblotting of primary murine myeloid cells (CD11b+) and Lewis lung carcinoma (LLC) cells with anti-myosin heavy chain A, B and C or HSP90 antibodies. (B) mRNA expression of Myh9, Myh10 and Myh14 in myeloid cells. (C) Effect of Myh9 and Myh10 siRNA on Myh9 expression. (D-E) Quantification (D) and Facs profiles (E) of VCAM-Fc binding to Myh9 and Myh10 siRNA transfected myeloid cells. (F) Cell adhesion to VCAM of Myh9 and Myh10 siRNA transfected myeloid cells. (G) Effect of Myh9 and Myh10 siRNA on Rap1 activation by SDF-1α in myeloid cells. (H) Effect of the myosin ATPase inhibitor blebbistatin on cytokine and p110γCAAX stimulation of myeloid cell adhesion to VCAM-1. (I) Immunofluorescence detection of integrin α4 (green) and myosin (red) in SDF1- bead stimulated *Mlck210-/-* myeloid cells that were transfected with WT or kinase dead *MLCK210* cDNA. Nuclei were detected with Dapi (blue). Data are represented as mean +/- SEM; n=4 for all conditions, $p<0.05$ unless otherwise defined.

adhesion was suppressed by W7 but not the PKC inhibitor (Supplementary Figure 3B), indicating a role for calmodulin in MLCK210-dependent integrin activation.

As MLCK210 expression in myeloid cells is required for myosin light chain phosphorylation and for Rap1 activation, our results suggest myosin could play a critical role in integrin activation. In fact, myosin has recently been suggested to serve as a scaffold for anchoring signaling proteins at the membrane[24]. We found that primary murine myeloid cells express non-muscle myosin heavy chain MHCIIA (encoded by Myh9) but not MHCIIB (encoded by Myh10) or MHCIIC (encoded by Myh14) (Figure 5A-B). Myh9 siRNA but not Myh10 siRNA, inhibited Myh9 expression, and prevented cytokine stimulated integrin $\alpha 4$ activation, as measured by VCAM-Fc binding to SDF-1a but not Mn2+ stimulated myeloid cells (Figure 5C-E). Similarly, Myh9 siRNA but not Myh10 siRNA prevented cytokine-stimulated integrin $\alpha 4$ mediated (Figure 5F). Myh9 siRNA also prevented Rap1 activation by SDF-1α (Figure 5G). Importantly, blebbistatin, a myosin-selective ATPase inhibitor,[25] suppressed cytokine and p110γCAAX stimulation of myeloid cell adhesion to VCAM-1, indicating that myosin catalytic activity promotes cell adhesion (Figure 5H)., Integrin $\alpha 4$ co-clustered with myosin (red) in SDF-1α bead stimulated myeloid cells in *Mlck210-/-* myeloid cells expressing WT but not kinase dead MLCK210, indicating that MLCK210 catalytic activity promotes myosin-integrin interactions (Figure 5I). Additionally, myosin, Rap1 and MLCK210 co-clustered in cells expressing active but not kinase dead MLCK210 (Supplementary Figure 3C). Together, these results indicate that MLCK210 phosphorylates and activates myosin, leading to clustering of adaptor and cytoskeletal proteins that are required to activate integrin.

MLCK210 mediates tumor inflammation and progression

Since MLCK210 is required for integrin activation in myeloid cells, we speculated that *Mlck210-/-* myeloid cells would exhibit defects in trafficking into sites of tumor inflammation in vivo. *Mlck210-*

/- myeloid cells, like *p110γ-/-, Rap1a-/-* and integrin α4Y991A myeloid cells[7], exhibited defective recruitment to Lewis lung carcinoma tumors (LLC) but not spleens within 2 h and up to 24h after adoptive transfer into animals with tumors (Figure 6A). Short term myeloid cell recruitment to LLC tumors was also suppressed when *Mlck* was knocked down by *Mlck* siRNA expression in adoptively transferred myeloid cells (Figure 6B). Lung carcinoma (LLC) tumor volumes and weights were substantially impaired in *Mlck210-/-* mice compared to WT mice, as were tumor volumes and incidence of metastases in mice bearing pancreatic ductal carcinomas (PDAC) (Figure 6C-F). Tumor growth, as measured by volume and weight was also suppressed in mice reconstituted with *Mlck210-/-* but not WT bone marrow (Figure 6G-I; Supplementary Figure 4A). Residual tumors in mice bearing *Mlck210-/-* bone marrow were necrotic compared to WT tumors (Figure 6J). As myeloid cell recruitment to tumors was suppressed in mice with *Mlck210-/-* bone marrow (Figure 6K-L), and inhibition of myeloid cell recruitment to LLC tumors promotes T cell recruitment and activation[12,25], these results suggest that loss of myeloid cell Mlck210 activity could lead to an improved immune response in tumors. Importantly, tumor growth and inflammation were suppressed in mice treated with the MLCK inhibitor MW01-022-AZ (Figure 6M-P; Supplementary Figure 4B). Taken together, these results indicated that myeloid cell MLCK210 plays a significant role in regulating tumor inflammation in vivo by promoting myosin mediated integrin activation and myeloid cell recruitment.

Figure 6

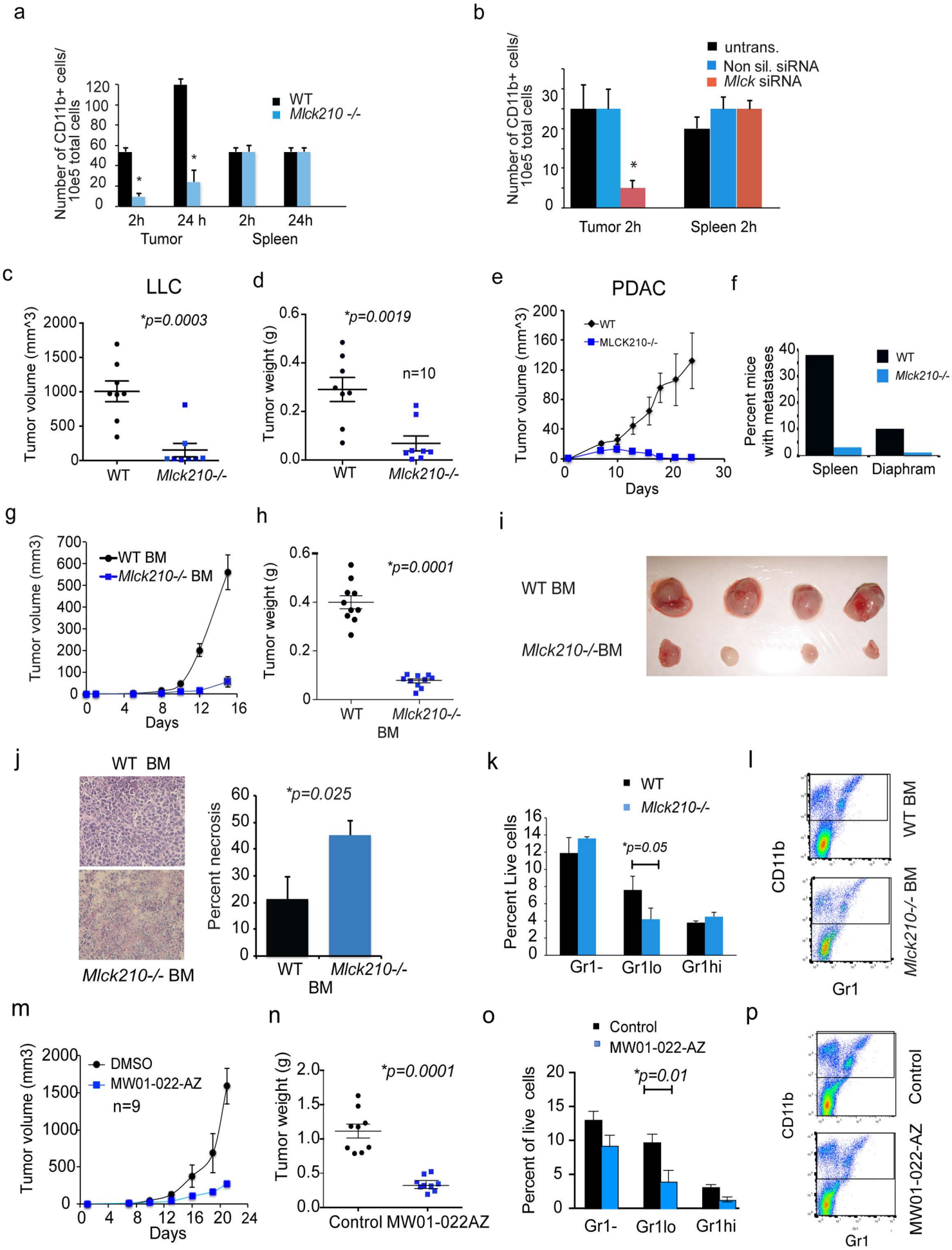
a
Number of CD11b+ cells/ 10e5 total cells
WT
Mlck210 -/-
2h
24 h
2h
24h
Tumor
Spleen
b
untrans.
Non sil. siRNA
Mlck siRNA
Tumor 2h
Spleen 2h
c
LLC
*p=0.0003
Tumor volume (mm^3)
WT
Mlck210-/-
d
*p=0.0019
n=10
Tumor weight (g)
e
PDAC
MLCK210-/-
Days
f
Percent mice with metastases
Spleen
Diaphram
g
WT BM
Mlck210-/- BM
Tumor volume (mm3)
h
*p=0.0001
BM
i
WT BM
Mlck210-/-BM
j
WT BM
Mlck210-/- BM
*p=0.025
Percent necrosis
k
*p=0.05
Percent Live cells
Gr1-
Gr1lo
Gr1hi
l
CD11b
Gr1
m
DMSO
MW01-022-AZ
n=9
n
*p=0.0001
Control
MW01-022AZ
o
*p=0.01
Percent of live cells
p

Figure 6: MLCK210 promotes inflammation and tumor growth (A) Number of FITC-labelled WT and *Mlck210*-/- CD11b+ cells in tumors 2-24h after adoptive transfer into mice. (B) Number of FITC-labelled control and *Mlck210* siRNA transfected CD11b+ cells in tumors 2h after adoptive transfer into mice. (C-D) Mean +/- SEM tumor (C) volume and (D) weight of LLC tumors in WT (n=10) and *Mlck210-/-* mice (n=10). (E) Time course of pancreatic ductal adenocarcinoma tumor growth in WT and *Mlck210-/-* tumors. (F) Percent mice with metastases from E. (G-H) Tumor volumes (G) and weights (H) and images (I) of LLC tumors in WT mice transplanted with bone marrow from WT (n=10) or *Mlck210-/-* mice (n=10). (J) Histographs of H&E stained tumor sections from mice transplanted with WT or *Mlck210-/-* bone marrow and graph of percent necrosis observed in tumor sections. (K-L) Quantification (K) and Facs profiles (L) of CD11b+ myeloid cells in WT and *Mlck210-/-* BM transplanted tumors. (M-P) Effect of MW01-022AZ on LLC (M) tumor volume and (N) tumor weight. (O-P) Quantification (O) and Facs profiles (P) of CD11b+ myeloid cells in control and MW01-022AZ treated tumors. Data are represented as mean +/- SEM; n=4 for all conditions, $p<0.05$ unless otherwise defined.

Discussion

We identified two high molecular weight proteins that co-immunoprecipitate with integrin $\alpha 4\beta 1$ in cytokine-stimulated myeloid cells. The studies presented here focus on the role of one of these, a high molecular weight form of myosin light chain kinase, MLCK210, that we found promotes myosin-dependent, Rap1-mediated integrin α4β1 activation. We show here that MLCK210 deletion, knockdown and inhibitors suppressed integrin activation and adhesion. Our studies showed that Rap1 activation is impaired in MLCK210-/- myeloid cells and that expression of activated Rap1, but not activated PI3Kγ, restored adhesive functionality to *Mlck210-/-* cells. These results indicate that MLCK210 acts downstream of PI3Kγ but upstream of Rap1. As myeloid cells lacking MLCK210 exhibit defects in integrin activation despite high expression levels of the non-muscle MLCK108 isoform, these results suggest that the unique N-terminal domain of MLCK210 plays a role in promoting integrin activation. Importantly, inflammation and tumor growth were substantially impaired in *Mlck210-/-* mice and in mice transplanted with *Mlck210-/-* bone marrow. As these results are similar to those observed in PI3Kγ-/- and integrin $\alpha 4$Y991A mutant mice[11-12], our studies indicate that MLCK210 likely plays a significant role in integrin activation in vivo.

Our studies show that MLCK210 expression in myeloid cells is required for MLC phosphorylation and for Rap1 activation, suggesting that the MCLK substrate myosin could play a critical role in integrin activation. Indeed, knockdown of Myh9, the major myosin isoform expressed in myeloid cells, as well as the myosin ATPase inhibitor blebbistatin inhibited integrin activation and adhesion. Prior studies showed that integrin $\alpha 4$-myosin interactions promote $\alpha 4$-mediated activation in transfected Chinese Hamster Ovary cells[28] and that myosin IIA-Rap1 interactions can promote Rap1-dependent integrin activation in fibroblasts[29].

Activation of integrin α4β1 by inside-out signaling promotes leukocyte extravasation from the vasculature[11-12]. Integrin activation depends on Rap1[6-7] and its effector protein RIAM, which localizes talin to the membrane[30-32]. Talin binds integrin β chain cytoplasmic tails, resulting in an allosteric increase in ligand binding affinity[30-32]. Paxillin binding to the integrin α4 cytoplasmic tail promotes integrin activation, adhesion and trafficking of lymphocytes and myeloid cells[8,33]. We showed here that integrin α4β1, MLCK210, talin and paxillin are all colocalized in cytokine-stimulated myeloid cells and that MLCK210 expression is necessary to promote Rap1 and paxillin co-localization with α4 integrin. Our data show that MLCK210 catalytic activity is required to promote integrin clustering and adhesion, as catalytically active MLCK210 but not inactive MLCK210 co-localizes with α4β1 and restores integrin clustering and adhesion to *Mlck210-/-* cells. Furthermore, MLCK210 phosphorylates myosin light chain, thereby inducing myosin ATPase activity and integrin activation in myeloid cells. The unique N-terminal head group of MLCK210 has been shown to target this kinase to the membrane and to actin filament[34], suggesting that MLCK210 may promote integrin activation by facilitating colocalization of integrin, signaling proteins and cytoskeletal components (see model, Supplementary Figure 4B).

Integrin cytoplasmic tails play critical roles in integrin activation. Integrin alpha and beta subunit cytoplasmic tails interact with each other through salt bridges between the membrane proximal GFKKR motif of the alpha subunit and the membrane proximal HDRRE motif of the beta chain[35-39]. R→A mutations in the GFFKR sequence in the cytoplasmic tails of α4, αIIb and αL constitutively activate these integrins[40]. Disruption of this salt bridge forces the cytoplasmic tails apart and alters extracellular domain conformations to increase ligand-binding affinity. The interaction of talin with NPxY sites in integrin β chain cytoplasmic tails also alters the packing of transmembrane domains and activates integrins[41]. Talin binding is facilitated by Rap1 activation, which promotes Rap1 effector protein RIAM to localize talin near the membrane[8]. Paxillin-binding

to the integrin α4 cytoplasmic tail also enhances integrin activation, as a Y→A mutation of the Y991 paxillin-binding site to A991 reduces talin binding and inhibits adhesion and trafficking of lymphocytes and myeloid cells[9-11]. Our studies here show that MLCK210 also play a key role in activating integrin $\alpha 4\beta 1$ by promoting myosin dependent Rap1 activation and localization and subsequent Talin and Paxillin binding to the integrin cytoplasmic tail, thereby contributing to cancer progression. A previous study described a role for MLCK in $\beta 2$ integrin activation, those studies described a myosin-independent role for low molecular weight MLCK in beta subunit integrin activation[42]. In contrast, our studies demonstrate a previously undescribed role for a high molecular weight variant of MLCK, MLCK210, in mediating integrin activation, inflammation and cancer progression.

Author contributions

Immunoprecipitations, silver-staining and proteomics were performed by Sang Won Kang and Michael C. Schmid. All other experiments were performed by Michael C. Schmid. Data analysis was performed by Michael C. Schmid, Megan M. Kaneda and Judith A. Varner. Mlck210-/- mice, MW01-22AZ and MLCK210 constructs were provided by D. Martin Watterson. The authors would like to thank Joan Manglicmot and Xiaodan Song for technical assistance.
Present address for Michael C. Schmid: M.Schmid@liverpool.ac.uk.

Declaration of Interests

The authors declare no competing interests.

Data availability

The datasets generated during and/or analyzed during the current study are available from the corresponding author on reasonable request.

Supplemental Figure 1

a

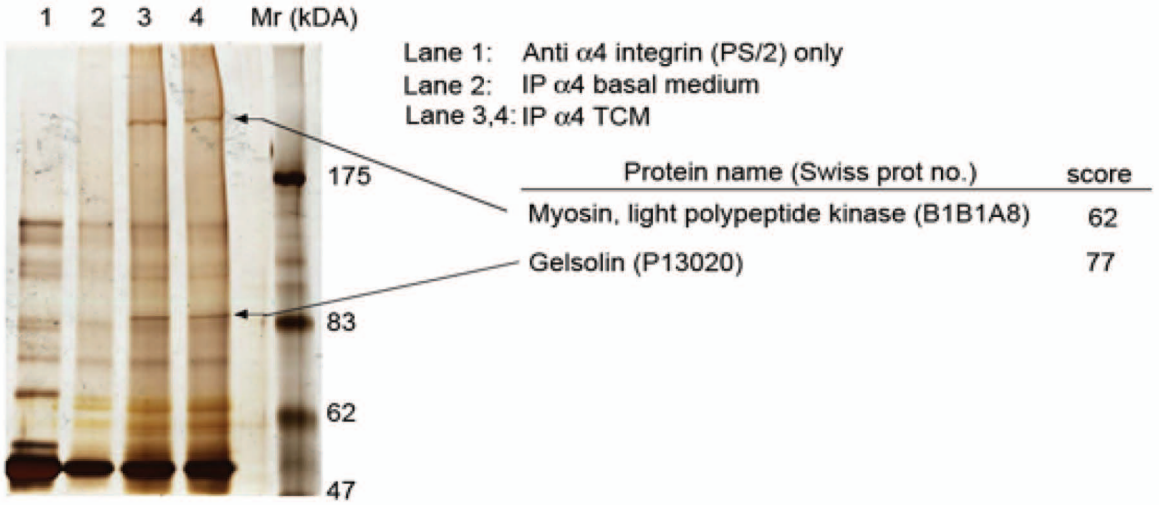

b

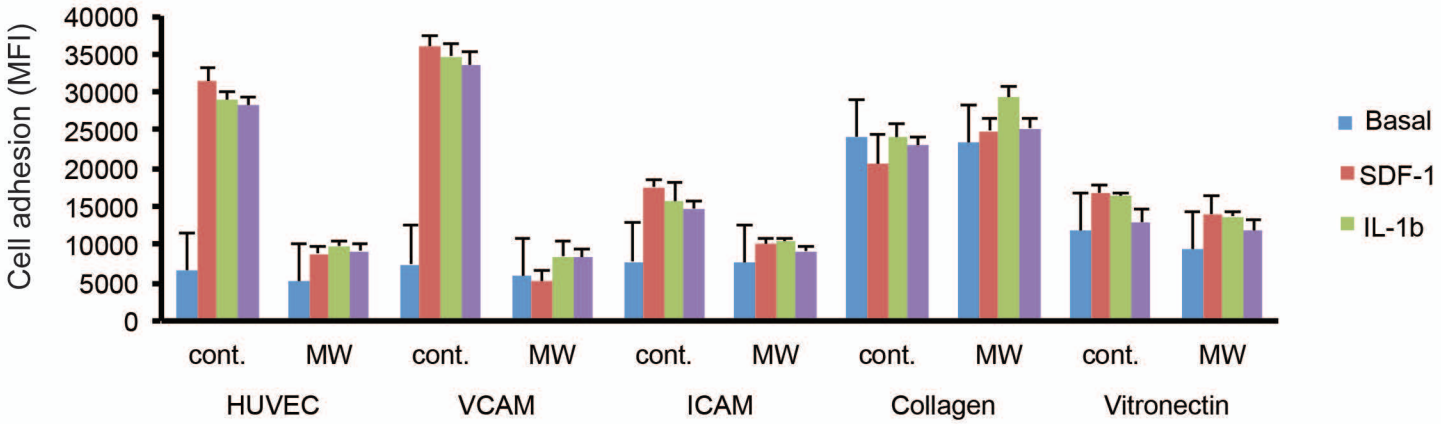

c

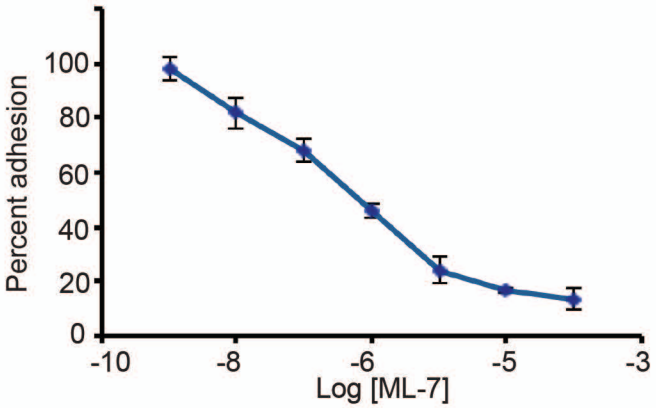

d

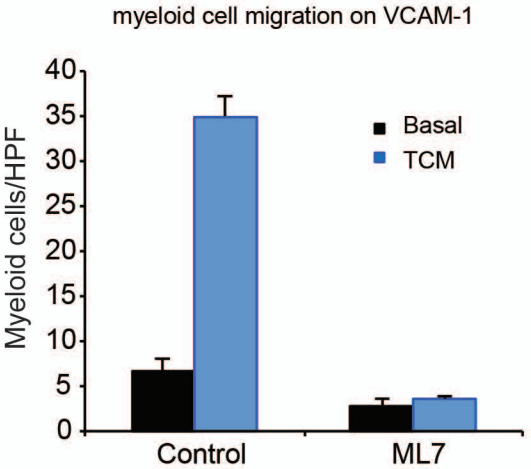

Supplementary Figure 1: *Mlck210* is required for myeloid cell integrin $\alpha 4$ activation.

(A) Silver stained gel from integrin $\alpha 4$ immunoprecipitates of basal and TCM stimulated myeloid cells. (B) Effect of the MLCK210 inhibitor MW01-022AZ on cytokine-stimulated myeloid cell adhesion to HUVEC, VCAM-1, ICAM-1, collagen or vitronectin. (C) Titration of the MLCK inhibitor ML-7 on myeloid cell adhesion to VCAM-1. (D) Effect of ML-7 on myeloid cell migration toward basal medium or LLC tumor conditioned medium. Data are represented as mean +/- SEM; n=4 for all conditions, $p<0.05$ unless otherwise defined.

Supplemental Figure 2

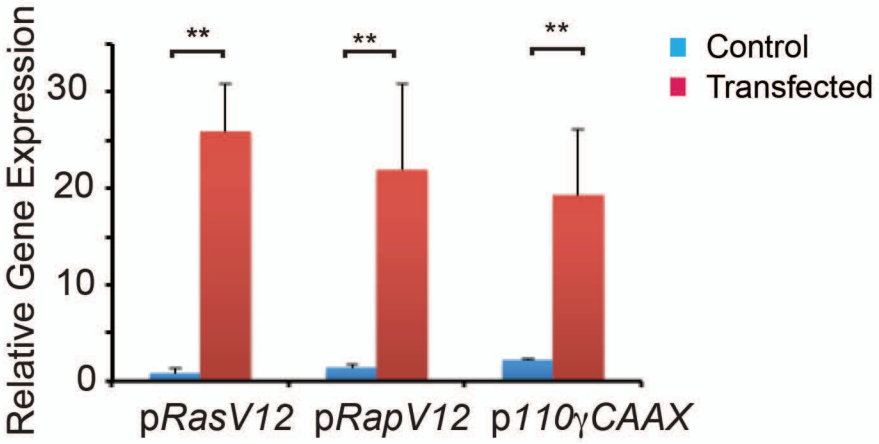

Supplementary Figure 2: Validation of transgene expression.

RT-PCR to detect expression of RasV12, RapV12 and p110γCAAX in myeloid cells that were transiently transfected with pRasG12V, pRapG12V or p110γCAAX. Data are represented as mean +/- SEM; n=3 for all conditions, $p<0.05$ unless otherwise defined.

Supplemental Figure 3

A

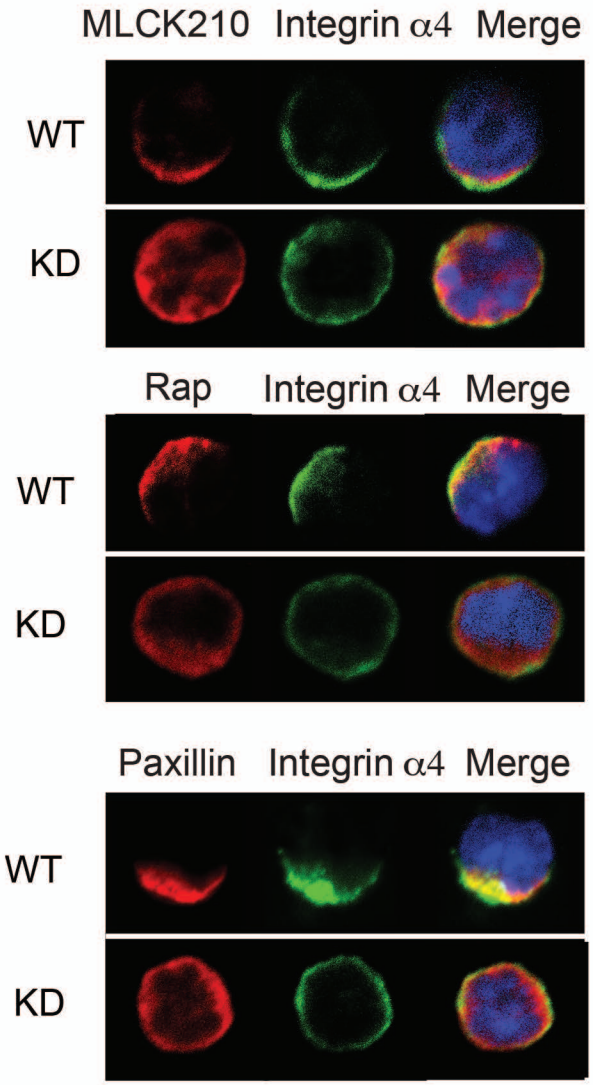

C

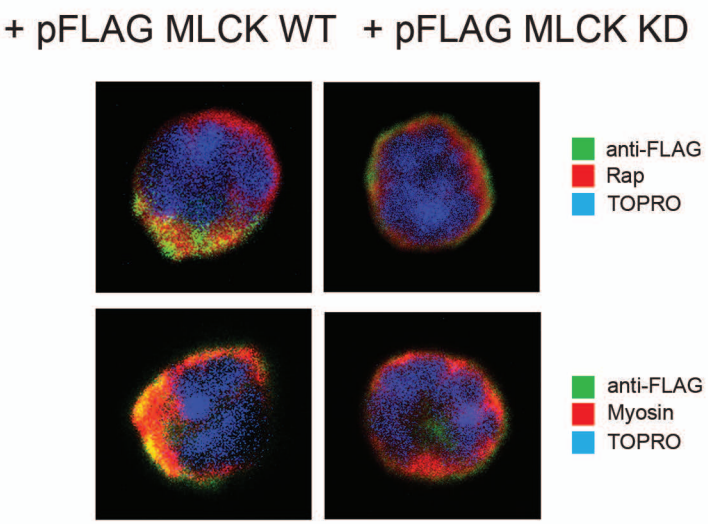

B

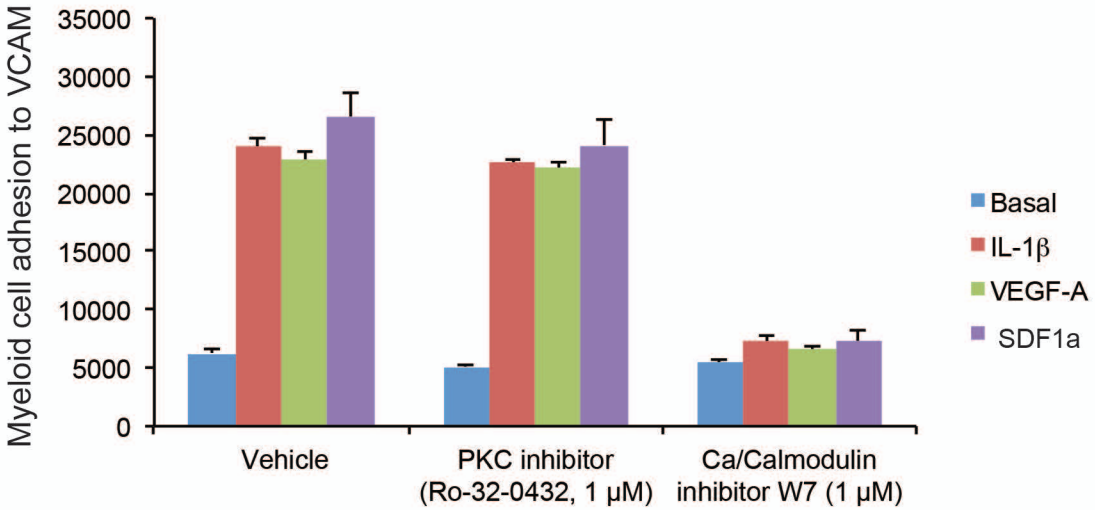

Supplementary Figure 3: Catalytically activity of MLCK210 is required for integrin α4 association with the cytoskeleton.

(A) Co-localization and co-clustering of integrin α4 and MLCK210, Rap1, and Paxillin in WT but not catalytically inactive (kinase dead, KD) transfected *Mlck210-/-* myeloid cells. (B) Effect of the PKC inhibitor R0-32-0432, the calcium/calmodulin inhibitor W7 and vehicle on cytokine stimulated myeloid cell adhesion to VCAM-1. (C) Co-localization and co-clustering of myosin, Rap1 and MLCK210 in WT but not catalytically inactive (kinase dead, KD) transfected *Mlck210-/-* myeloid cells.

Supplemental Figure 4

a

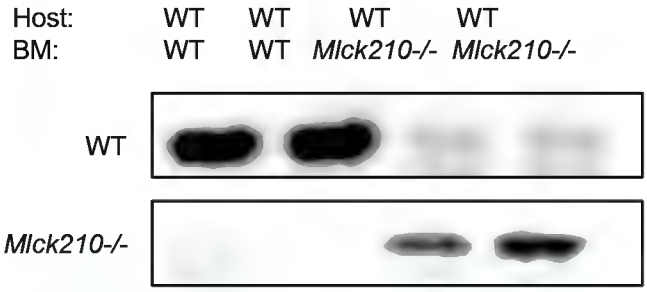

b

c

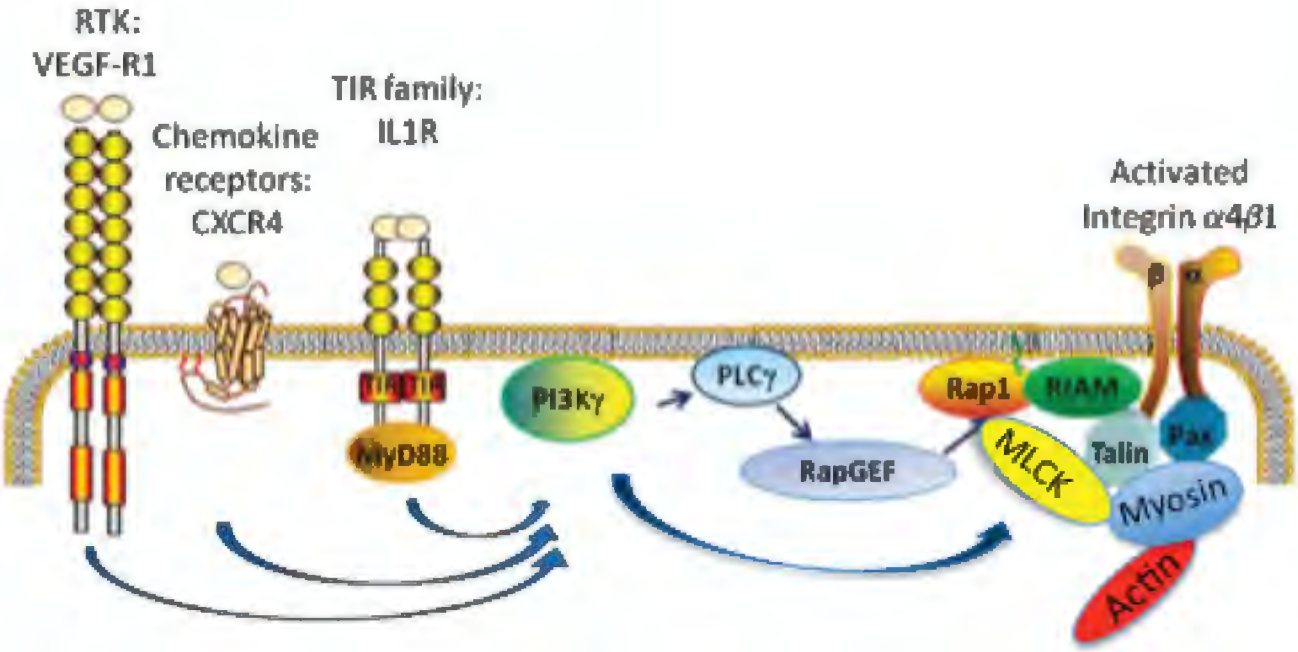

Supplementary Figure 4: *Mlck210* deletion suppresses tumor growth.

(A) Genomic PCR to detect WT *Mlck*210 and the *Mlck210* deletion mutant in peripheral blood cells from BMT transplanted mice. (B) Images of control and MW01-22AZ treated tumors. (C) Model of integrin activation demonstrating that cytokine stimulation activates a pathway whereby PI3Kγ induces *Mlck210* and myosin activation and co-localization with Rap1, resulting Rap1-mediated integrin α4 conformation changes and interaction of the integrin with the actin cytoskeleton.

References

1. Barrat, F.J., et al. Interferon target-gene expression and epigenomic signatures in health and disease. *Nat Immunol* **20,** 1574–1583 (2019).

2. Pathria, P., Louis, T.L. & Varner ,J.A. Targeting Tumor-Associated Macrophages in Cancer. *Trends Immunol* **40**,310-327 (2019).

3. Pons, S., et al. Immune Consequences of Endothelial Cells' Activation and Dysfunction During Sepsis. *Crit Care Clin* **36**, 401-413 (2020).

4. Todoric, J., Antonucci, L., Karin, M. Targeting Inflammation in Cancer Prevention and Therapy. *Cancer Prev Res* **9**, 895-905 (2016).

5. Schmid, M.C. & Varner, J.A. Myeloid cells in tumor inflammation. *Vasc Cell* **4**, 14 (2012).

6. Lagarrigue, F., Kim, C., & Ginsberg, M.H. The Rap1-RIAM-talin axis of integrin activation and blood cell function. *Blood* **128**, 479-87 (2016).

7. Schmid, M.C., et al. PI3-kinase γ promotes Rap1a-mediated activation of myeloid cell integrin α4β1, leading to tumor inflammation and growth. *PLoS One* **8**, e60226 (2013).

8. Lagarrigue, F., et al. Talin-1 is the principal platelet Rap1 effector of integrin activation. *Blood* **136**,1180-1190 (2020).

9. Féral, C.C., et al. Blocking the alpha 4 integrin-paxillin interaction selectively impairs mononuclear leukocyte recruitment to an inflammatory site. *J Clin Invest* **116**, 715-23 (2006).

10: Alon, R., et al. Alpha4beta1-dependent adhesion strengthening under mechanical strain is regulated by paxillin association with the alpha4-cytoplasmic domain. *J Cell Biol* **171**,1073-84 (2005).

11. Schmid, M.C., et al. Combined blockade of integrin-α4β1 plus cytokines SDF-1α or IL-1β potently inhibits tumor inflammation and growth. *Cancer Res* **71**, 6965-75 (2011).

12. Schmid, M.C., et al. Receptor tyrosine kinases and TLR/IL1Rs unexpectedly activate myeloid cell PI3kγ, a single convergent point promoting tumor inflammation and progression. *Cancer Cell* **19**, 715-27 (2011).

13. Kudryashov, D.S., et al. Unique sequence of a high molecular weight myosin light chain kinase is involved in interaction with actin cytoskeleton. *FEBS Lett.* **463**, 67-71 (1999).

14. Wainwright, M.S., et al. Protein kinase involved in lung injury susceptibility: evidence from enzyme isoform genetic knockout and in vivo inhibitor treatment. *Proc Natl Acad Sci U S A*. **100**, 6233-8 (2003).

15. Fazal, F., et al. Critical role of non-muscle myosin light chain kinase in thrombin-induced endothelial cell inflammation and lung PMN infiltration. *PLoS One* **8**, e59965 (2013).

16. Rossi, J.L., Velentza, A.V., Steinhorn, D.M., Watterson, D.M. & Wainwright, M.S. MLCK210 gene knockout or kinase inhibition preserves lung function following endotoxin-induced lung injury in mice. *Am J Physiol Lung Cell Mol Physiol.* **292,** L1327-34 (2007).

17. Ralay Ranaivo H., et al. Protection against endotoxic shock as a consequence of reduced nitrosative stress in MLCK210-null mice. *Am J Pathol* **170**, 439-46 (2007).

18. Mirzapoiazova, T., et al. Non-muscle myosin light chain kinase isoform is a viable molecular target in acute inflammatory lung injury. *Am J Respir Cell Mol Biol.* **44**, 40-52 (2011).

19. Feldt, J., et al. Structure, regulation and related diseases of the actin-binding protein gelsolin. *Expert Rev. Mol. Med.* **20**, e7 (2019).

20. Means, A.R., Bagchi, I.C., VanBerkum, M.F., & Kemp, B.E. Regulation of smooth muscle myosin light chain kinase by calmodulin. *Adv Exp Med Biol.* **304**,11-24 (1991).

21. Kelkar, M., Bohec, P., & Charras, G. Mechanics of the cellular actin cortex: From signalling to shape change. *Curr Opin Cell Biol.* **66**, 69-78 (2020).

22. Bachmann, M., Kukkurainen, S., Hytönen, V.P., & Wehrle-Haller, B. Cell Adhesion by Integrins. *Physiol Rev.* **99**, 1655-1699 (2019).

23 Stefanini, L., & Bergmeier, W. RAP GTPases and platelet integrin signaling. *Platelets* **30**, 41-47 (2019).

24 Brito, C., & Sousa, S. Non-Muscle Myosin 2A (NM2A): Structure, Regulation and Function. *Cells* **9**,1590 (2020).

25. Straight, A.F., et al. Dissecting temporal and spatial control of cytokinesis with a myosin II Inhibitor. *Science* **299**, 1743-7 (2003).

26. Kaneda, M.M., et al. PI3Kγ is a molecular switch that controls immune suppression. *Nature* **539**, 437-42 (2016).

27. Behanna, H.A., Watterson, D.M., & Ralay Ranaivo, H. Development of a novel bioavailable inhibitor of the calmodulin-regulated protein kinase MLCK: a lead compound that attenuates vascular leak. *Biochim Biophys Acta*. **1763**,1266-74 (2006).

28. Rivera Rosado, L.A., Horn, T.A., McGrath, S.C., Cotter, R.J., & Yang, J.T. Association between α4 integrin cytoplasmic tail and non-muscle myosin IIA regulates cell migration. *J Cell Sci.* **124**, 483-92 (2011).

29. Arora, P.D., et al. Rap1 activation in collagen phagocytosis is dependent on nonmuscle myosin II-A. *Mol Biol Cell* **19**, 5032-46 (2008).

30. Lee HS, Lim CJ, Puzon-McLaughlin W, Shattil SJ, & Ginsberg MH. RIAM activates integrins by linking talin to ras GTPase membrane-targeting sequences. *J Biol Chem* **284**, 5119-27 (2009).

31. Lagarrigue, F., Kim, C., & Ginsberg, M.H. The Rap1-RIAM-talin axis of integrin activation and blood cell function. *Blood* **128**, 479-87 (2016).

32. Gingras, A.R., et al. Rap1 binding and a lipid-dependent helix in talin F1 domain promote integrin activation in tandem. *J Cell Biol.* **218**, 1799-1809 (2019).

33. Kukkurainen, S., et al. The F1 loop of the talin head domain acts as a gatekeeper in integrin activation and clustering. *J Cell Sci*.**133**, 239202 (2020).

34. Kudryashov DS, et al. Myosin light chain kinase (210 kDa) is a potential cytoskeleton integrator through its unique N-terminal domain. *Exp Cell Res*. **298**, 407-17 (2004).

35. Bittner, M., Gosslar, U., Luz, A., & Holzmann, B. Sequence motifs in the integrin alpha 4 cytoplasmic tail required for regulation of in vivo expansion of murine lymphoma cells. *J Immunol*. **161**, 5978-86 (1998).

36 De Melker, A.A., Kramer, D., Kuikman, I., & Sonnenberg, A. The two phenylalanines in the GFFKR motif of the integrin alpha6A subunit are essential for heterodimerization. *Biochem J.* **328**, 529-37 (1997).

37 Lu, C.F., & Springer, T.A. The alpha subunit cytoplasmic domain regulates the assembly and adhesiveness of integrin lymphocyte function-associated antigen-1. *J Immunol* **159**, 268-78 (1997).

38 De Melker, A.A., & Sonnenberg, A. The role of the cytoplasmic domain of alpha 6 integrin in the assembly and function of alpha 6 beta 1 and alpha 6 beta 4. Eur *J Biochem* 241, 254-64 (1996) .

39 Kassner, P.D., Kawaguchi, S., & Hemler, M.E. Minimum alpha chain cytoplasmic tail sequence needed to support integrin-mediated adhesion. *J Biol Chem* **269**, 19859-67 (1994).

40. Imai, Y., et al. Genetic perturbation of the putative cytoplasmic membrane-proximal

salt bridge aberrantly activates alpha(4) integrins. *Blood* **112**, 5007-15 (2008).

41. García-Alvarez, B., et al. Structural determinants of integrin recognition by talin. Mol *Cell* **11**, 49-58 (2003).

42. Xu, J., et al. Nonmuscle myosin light-chain kinase mediates neutrophil transmigration in sepsis-induced lung inflammation by activating beta2 integrins. *Nat Immunol* **9**, 880-6 (2008).

Materials and Methods

Reagents

MW01-022AZ was provided by D.M. Watterson, Northwestern University. Flag-tagged *Mlck210* and Flag-tagged kinase dead *Mlck210* expression constructs were provided by D.M. Watterson, Northwestern University. RasV12, RapV12, p110γCAAX pcDNA plasmids were previously described[ref]. ML-7 was from Selleck Chemicals. C57BL/6 LLC cells were obtained from the American Type Culture Collection (ATCC). LMP pancreatic tumor cells were previously described[ref]. All cells were verified by RNA sequencing or RT-PCR. All cell lines were tested for mycoplasma and mouse pathogens.

Animals and Human Subjects

Mlck210-/- animals were from D.M. Watterson, Northwestern University. C57BL6 animals were purchased from Jackson Laboratories and bred at the University of California San Diego. All animal experiments were performed with approval of the Institutional Animal Care and Use Committee of the University of California San Diego. Use of donated human peripheral blood cells from the San Diego Blood Bank was approved by the Institutional Review Board for human subjects research of the University of California, San Diego.

Purification of myeloid cells

Myeloid cells were purified from murine bone marrow or human buffy coats obtained from the San Diego Blood Bank using anti-CD11b magnetic bead affinity chromatography according to manufacturer's directions (Miltenyi Biotec). The purity of the purified CD11b+ cell population was assessed by Facs analysis.

Adhesion assays

1 X 10^5 calcein-AM labelled CD11b+ cells were incubated on 48 well culture plates containing endothelial cell monolayers (HUVEC) or coated with 5µg/ml recombinant soluble VCAM-1 (R&D Systems), ICAM-1 (R&D Systems), vitronectin, or collagen for 20min at 37ºC in basal media, culture media from Lewis lung carcinoma cells (TCM) or DMEM containing 200ng/ml SDF1α, IL-1β, IL-6, TNFα or VEGF-A (R&D Systems) without or with 1µM inhibitors directed against MLCK (ML-7 or MW01-022AZ), PKC (Ro-32-0432), calcium/calmodulin (W7) or myosin (Blebbistatin). Additionally, CD11b+ myeloid cells from WT, *Rap1-/-, p110γ -/-,* and *Mlck210-/-* mice as well as *Mlck, Myh9, Myh10* and non-silencing siRNA-transfected and RasV12, RapV12 and p110γCAAX-transfected cells were similarly incubated for 20min on 5µg/ml rsVCAM-1. After washing three times with warmed medium, adherent cells were quantified using a plate fluorimeter (TECAN).

Ligand binding assay

1x10^6 WT or *Mlck210-/-* murine CD11b+ cells or CD11b+ cells transfected with *Mlck*, *Myh9, Myh10* or non-silencing siRNAs and myeloid cells treated with ML-7 or MW01-022AZ were incubated with 200ng/ml IL-1β, SDF-1α, IL-6, TNFα, VEGF-A or medium together with 1mg/ml mouse VCAM-1/human-Fc fusion protein (R&D Systems). Cells were washed twice and incubated with donkey anti-human Fc antibody (Jackson Immunoresearch) then analyzed by flow cytometry. Mean fluorescence intensity of treated cells was compared to that of unstimulated cells (basal).

HUT21 integrin activation assay

To quantify integrin activation, 2.5 X 10^6 MW01-022AZ or control treated human myeloid cells/ml were incubated in culture medium containing 10µg/ml normal human immunoglobulin (12000C, Caltag Laboratories, Burlingame, CA) for 45 min on ice. These cells were then incubated in 200

ng/ml SDF-1α or 1mM Mn2+ in the presence or absence of 2.5µg HUTS21 (β1 activation epitope, BD-Bioscience), P4C10 (total β1, EMD/Millipore), or IgG2 control for 10min at 37°C, followed by Alexa 488 goat-anti-mouse antibodies for 20min on ice. Bound antibody was quantified by flow cytometry.

siRNA and plasmid transfections

Purified CD11b+ cells were transfected with 2 µg/ 1 X 10^6 cells pcDNA 3.1 p110□CAAX, pcDNA3.1 RasV12, pcDNA3.1 RapV12, or pGFPMax (Lonza) using Lonza Mouse Macrophage Nucleofection Kits. Alternatively, CD11b+ cells were transfected with 100 nM of siRNA targeting *Mlck* (Mm_Mylk_1 and Mm_Mylk_2), *Myh9 (*Mm_Myh9_1 and Mm_Myh9_2), *Myh10* (Mm_Myh10_1 and Mm_Myh10_2) or non-silencing siRNA (Ctrl_AllStars_1) from Qiagen. After transfection, cells were maintained for 24 h in culture media containing 20% serum. Each siRNA was tested individually for efficient knockdown of protein expression and for inhibition of adhesion or ligand binding. To control for off-target effects of siRNAs, only previously validated siRNAs were used.

Gene expression

Total RNA was isolated from primary myeloid cells using RNeasy Kit (Qiagen). cDNA was prepared from 500ng RNA from each sample and qPCR was performed using primer sets for Mylk *(Mm_Mylk_1_SG)*, *Myh9 (Mm_Myh9_1_SG)*, *Myh10 (Mm_Myh10_1_SG)*, *Myh14 (Mm_Myh14_1_SG)* from Qiagen (QuantiTect Primer Assay). GAPDH (*Gapdh*) sense primers 5′CATGTTCCAGTATGACTCCACTC3′ and anti-sense primers 5′GGCCTCACCCCATTTGATGT3'. Relative expression levels were normalized to *Gapdh* expression according to the formula [2^- (Ct *gene of interest* – Ct *gapdh*)][49].

Rap1 activation assay

Rap activity was measured at 37°C after stimulation with basal medium or medium containing 200ng/ml SDF-1α (R&D Systems) for 3 minutes. GTP-Rap was purified from 1 mg cell lysate by addition of RalGDS-GST fusion proteins and glutathione-conjugated sepharose beads. using a RapGTPase pulldown assay kit (Thermo Scientific). GTP-Rap and total Rap were detected by immunoblotting with anti-Rap1 antibodies as previously described.

Immunoprecipitation

Myeloid cells were treated with either basal media or TCM at 37°C, rinsed with cold PBS and lysed in Tris-buffered saline containing 1% CHAPS, 20mM β-glycerophosphate, 1mM Na3VO4, 5mM NaF, 100ng/ml microcystin-LR, and protease inhibitor cocktail. After centrifugation, integrin α4β1 was immunoprecipitated as follows: 1mg total protein was precleared with 10µl protein G conjugated Dynabeads (Invitrogen) for 1hr at 4°C with rotation. Cleared lysates were incubated with 5µg of rat anti-mouse integrin α4 (PS2) at 4°C for 2h, then with 30µl of protein G conjugated Dynabeads for 2h with rotation. Beads were washed three times with 1ml cold PBS containing protease inhibitor cocktail. Protein precipitates were electrophoresed on 10% SDS-PAGE gels and immunoblotted with rat anti-mouse α4 antibodies Protein precipitates were electrophoresed and immunoblotted with anti-integrin α4 (C-20, Santa Cruz Biotechnology), anti-paxillin (H-114, Santa Cruz Biotechnology), or anti-talin (Clone TD77, Chemicon) or MLCK210 (sc-22223, Santa Cruz).

Immunoblotting

Total myeloid cell lysates were electrophoresed on 10% SDS-PAGE gels and immunoblotted to detect MLCK210 (sc-22223, Santa Cruz), integrin α4 (EPR1355Y, Epitomics/Abcam), integrin b3 (), pSer18/pThr19 myosin light chain (Cell Signaling 3674), myosin light chain 2 (Cell Signaling

3672), pAkt (244F9, Cell Signaling) and Akt (11E7, Cell Signaling), Rabbit anti-Flag tag (F7425, Sigma) and myosin heavy chains A (Cell Signaling 3403), B (Cell Signaling 3404) and C (Cell Signaling 3405).

In vivo myeloid cell trafficking studies

$5x10^6$ CFSE labelled CD11b+ cells from C57BL/6 WT and *Mlck210-/-* mice or $5x10^6$ CFSE labelled *Mlck* and non-silencing siRNA transfected CD11b+ cells were injected intravenously into WT mice bearing subcutaneous d14 LLC tumors. Fluorescent cells accumulating in tumors and spleens were quantified at 2h and 24h after inoculation by flow cytometry of single cell preparations of tumors.

Tumor studies

C57BL/6 LLC cells and LMP pancreatic tumor cells were cultured in antibiotic- and fungicide-free DMEM media containing 10% serum; cells tested negative for mycoplasma. 5 $X10^5$ LLC or LPM cells were injected subcutaneously into syngeneic female 6-to 8-week old wildtype C57Bl6 or *Mlck210-/-* mice (n=8-10). Tumors dimensions were recorded at regular intervals. Tumors were excised at 21 days. Tumor weights were obtained, and tumors were cryopreserved in O.C.T., cryosectioned and stained with hematoxylin and eosin. LLC tumors were analyzed for areas of necrosis using Metamorph software (Molecular Devices). In some experiments, animals were normalized seven days after tumor cell inoculation in to two groups, each with a starting volume of $10mm^3$. Animals were then treated with daily i.p. injections of either 0.1 mg MW01-022AZ in 1% DMSO or vehicle (1% DMSO) control.

Bone marrow transplantation and tumor studies

Bone marrow derived cells were aseptically harvested from 6-8 week-old wildtype or *Mlck210-/-* female mice in the C57Bl6 background by flushing leg bones of euthanized mice with phosphate

buffered saline containing 0.5% BSA and 2mM EDTA, incubating cells in red cell lysis buffer (155mM NH_4Cl, 10mM $NaHCO_3$ and 0.1mM EDTA) and centrifuging over Histopaque 1083. Approximately $5X10^7$ BMDC were purified by gradient centrifugation from the femurs and tibias of a single mouse. Two million cells were intravenously injected into tail veins of lethally irradiated (1000 rad) 6-week old syngeneic recipient wildtype mouse. After 4 weeks of recovery and confirmation of successful transplant, $5 X10^5$ tumor cells were inoculated into BM transplanted animals (n=8) and tumor growth was monitored as described above. Successful engraftment of mutant bone marrow was assessed by isolating genomic DNA from peripheral blood cells of fully recovered bone marrow-transplanted mice. Engraftment of *Mlck210-/-* BM was assessed by PCR.

Quantification of myeloid cells in tissues by flow cytometry

To quantify myeloid cells in tissues, tumors were excised, minced and digested to single cell suspensions for 1h at 37°C in 5ml of Hanks Balanced Salt Solution (HBSS, GIBCO) containing 1mg/ml Collagenase type IV, 10µg/ml Hyaluronidase type V and 20 units/ml DNase type IV (Sigma). Red blood cells were solublized with RBC Lysis Buffer (ThermoFisher). Single cell suspensions (10^6 cells in 100 µL total volume) were incubated with 0.5µg/ml propidium iodide and then with Fc-blocking reagent (BD) or serum followed by anti-CD11b-APC (M1/70) and anti-Gr1-FITC (RB6-8C5) (eBioscience/ThermoFisher). Facs analysis was performed using Flowjo software (Treestar, Inc).

MLCK activity assay:

Total bone marrow monocytic cells from WT and MLCK-/- mice were transfected with 2 ug of empty pcDNA3.1 plasmid, or pcDNA3.1 vector expressing FLAG-MLCK210-WT or FLAG-MLCK210-kinase dead gene protein (provided by Dr. Daniel Watterson, Northwestern University) using Nucleofection (LONZA). Transfected cells were cultured overnight at 37°C in RPMI + 20%

FBS + Pen/Strep. The next day, cells were serum starved for 6 h and then stimulated with 200 ng/ml SDF-1a (PeproTech) for 15 minutes or left untreated. Cells were solubilized in standard RIPA buffer containing protease and phosphatase inhibitor cocktail. MLCK activity was measured by immunoblotting to detect phosphorylation of Ser18/Thr19 on myosin light chain (MLC) (Cell Signaling, #3674, diluted 1/1000 in TBST + 5% BSA). Total MLC protein levels were detected by MLC2 antibody (Cell Signaling, #3672, 1:1/000 in TBST + 5% BSA). Efficient expression of MLCK constructs was confirmed using anti-FLAG antibody (M2, Sigma).

Cell Clustering

To induce integrin α4 activation on myeloid cells, purified myeloid cells were incubated with polystyrene microspheres (9.0μm diameter, Bangs Laboratories) that had been coated with 200ng/ml SDF-1α or 2% BSA overnight at 4°C. Cells were incubated with beads for 5 min at 37°C, then fixed in 1% paraformaldehyde. Cells were then immunostained with fluorochrome-conjugated anti-integrin α4 (R1/2, Biolegend), anti-paxillin (H-114, Santa Cruz), anti-talin (H-300, Santa-Cruz), anti-Rap1, myosin heavy chain IA (Cell Signaling 3403), rabbit anti-Flag (F7425, Sigma) and TOPRO-3 (Invitrogen). Samples were analyzed by Nikon CS1 spectral confocal on a Nikon TE2000E inverted microscope. Images were captured using Metamorph software.